

Universiteit
Leiden
The Netherlands

Studies on the pathogenesis of chronic kidney disease

He, J.

Citation
He, J. (2021, September 15). *Studies on the pathogenesis of chronic kidney disease*. Retrieved from https://hdl.handle.net/1887/3210130

Version:	Publisher's Version
License:	Licence agreement concerning inclusion of doctoral thesis in the Institutional Repository of the University of Leiden
Downloaded from:	https://hdl.handle.net/1887/3210130

Note: To cite this publication please use the final published version (if applicable).

Cover Page



Universiteit Leiden



The handle https://hdl.handle.net/1887/3210130 holds various files of this Leiden University dissertation.

Author: He, J.
Title: Studies on the pathogenesis of chronic kidney disease
Issue Date: 2021-09-15

Chapter 4

Leptin deficiency affects glucose homeostasis and results in adiposity in zebrafish

Junling He*, Yi Ding*, Natalia Nowik, Charel Jager, Muhamed N. H. Eeza, A. Alia, Hans J. Baelde, Herman P. Spaink.

*These authors contributed equally to this work

J Endocrinol. 2021 May;249(2):125-134.

Abstract

Leptin is a hormone which functions in the regulation of energy homeostasis via suppression of appetite. In zebrafish, there are two paralogous genes encoding leptin, called *lepa* and *lepb*. In a gene expression study, we found that the *lepb* gene, not the *lepa* gene, was significantly downregulated under the state of insulin-resistance in zebrafish larvae, suggesting that the *lepb* plays a role in glucose homeostasis. In the current study, we characterised *lepb*-deficient (*lepb*$^{-/-}$) adult zebrafish generated via a CRISPR-CAS9 gene editing approach by investigating whether the disruption of the *lepb* gene would result in the development of type 2 diabetes mellitus (T2DM) and diabetic complications. We observed that *lepb*$^{-/-}$ adult zebrafish had an increase in body weight, length and visceral fat accumulation, compared to age-matched control zebrafish. In addition, *lepb*$^{-/-}$ zebrafish had significantly higher blood glucose levels compared to control zebrafish. These data collectively indicate that *lepb*$^{-/-}$ adult zebrafish display the features of T2DM. Furthermore, we showed that *lepb*$^{-/-}$ adult zebrafish had glomerular hypertrophy and thickening of the glomerular basement membrane, compared to control zebrafish, suggesting that *lepb*$^{-/-}$ adult zebrafish develop early signs of diabetic nephropathy. In conclusion, our results demonstrate that *lepb* regulates glucose homeostasis and adiposity in zebrafish, and suggest that *lepb*$^{-/-}$ mutant zebrafish are a promising model to investigate the role of leptin in the development of T2DM and are an attractive model to perform mechanistic and therapeutic research in T2DM and its complications.

Introduction

Human leptin is a 16-kDa protein hormone which is predominantly secreted by adipocytes [1]. Leptin plays a role in diverse physiological processes including energy homeostasis [2], immune regulation [3,4], endocrine regulation [5], and reproduction [6,7]. Congenital leptin deficiency causes extreme obesity in children [8,9]. Rodents lacking the gene encoding leptin are commonly characterised by hyperphagia, obesity, insulin resistance and impaired glucose tolerance. For instance, *leptin*-deficient mice (*ob/ob* mice) exhibit the features of obesity and type 2 diabetic mellitus (T2DM) [10]. Growing evidence suggests that leptin treatment has a beneficial effect on glucose metabolism [11-14] and insulin resistance [15-18], indicating that leptin might be a crucial factor in the development of T2DM. However, the function of leptin in the pathogenesis of T2DM is still obscure.

Leptin and leptin receptor are highly conserved across mammalian species. The most widely used animal models in T2DM research are the congenial *leptin*- or *leptin* receptor-deficient rodent models, such as *ob/ob* and *db/db* mice. Besides, the basic structural features and intracellular signaling mechanisms of leptin and its receptor appear to be conserved throughout vertebrates [19]. Several studies have reported that administration of exogenous leptin in fish reduces food intake, indicating the conservation of the function of the leptin signaling system throughout vertebrates [20-22]. In recent decades, zebrafish have become a promising animal model with numerous advantages, including fast development and generation time, small size, easily accessible, and cost-effective. In zebrafish, there are two divergent leptin paralogues: *lepa* and *lepb*, and one leptin receptor gene (*lepr*) [23]. Michel et al. [24] demonstrated that *lepr*-deficient zebrafish larvae have increased numbers of β-cells and increased insulin mRNA expression, compared to control zebrafish larvae. They also found that the leptin receptor deficiency contributes to higher blood glucose levels in adult zebrafish. Their findings indicated that the regulation of glucose homeostasis by the leptin receptor is conserved across vertebrates. However, they observed no significant difference in the whole body adiposity phenotype between *lepr*-deficient zebrafish and control zebrafish at the adult stage. On the other hand, Chisada et al. [25] showed that the deletion of leptin receptor in medaka results in a modest increase in visceral fat accumulation compared to the wild type (WT) medaka fish. More recently, Audira et al. [26] found that *lepa*-deficient adult zebrafish display an obesity phenotype. Thus, there are some conflicting results in the literature regarding the relationship between disruption of leptin signaling and adiposity in zebrafish. In a previous study, our group found that the *lepb* gene, not the *lepa* gene, was significantly downregulated in zebrafish larvae under an insulin-resistance state, resulting from acute hyperinsulinemia, which suggests that *lepb*

plays a role in insulin homeostasis in zebrafish [27]. Since the roles of *lepa* and *lepr* in zebrafish have already been investigated by other groups, therefore, the focus in the current work is to study the function of the *lepb* gene in zebrafish at an adult stage to obtain more insights into the relationship between the leptin signaling pathway and T2DM.

This study aims to investigate whether *lepb* deficiency contributes to the development of T2DM in adult zebrafish. To address this question, we examined the body weight and length, blood glucose levels, and the body fat distribution in 1.5 years old $lepb^{-/-}$ adult zebrafish and compared them to age-matched WT controls. Furthermore, we examined the renal histopathologic changes of these zebrafish by performing hematoxylin and eosin (HE) or Periodic-acid Schiff (PAS) staining, and transmission electron microscopy (TEM) methods.

Methods and Materials

Animals

Zebrafish strains were handled in compliance with the local animal welfare regulations and maintained according to standard protocols (zfin.org). The use of adult zebrafish was approved by the local animal welfare committee (DEC) of the University of Leiden (license number: AVD1060020171767) and adhered to the international guidelines specified by the EU Animal Protection Directive 2010/63/EU.

The CRISPR-CAS9 gene editing approach was used to knock out the *lepb* in the ABTL zebrafish to generate the *lepb*-deficient zebrafish. The sgRNA CTACCCAATCCCGAGACCCC targeted the exon 2 in *lepb*. The *lepb* primer (for: 5'-*AGGAACTGGCCGTCTCACAG*-3'; rev: *5'-CGGGGAAGGCTGTTTCTTCTT-3'*) was used for *lepb*-deficient zebrafish genotyping. Sanger sequencing showed that a 7bp ($lepb^{7-/7-}$) or 8bp ($lepb^{8-/8-}$) stretch of nucleotides was missing in the *lepb* gene in two different mutant lines (Supplementary Fig. 1A). Both deletions resulted in a frameshift mutation of *lepb* (Supplementary Fig. 1B). The deletion of the *lepb* gene was in codon 110 in zebrafish, which is close to the non-sense mutation in codon 105 of the *leptin* gene of C57BL/6J *ob/ob* mice. In the C57BL/6J *ob/ob* mice, this mutation in the *leptin* gene leads to a truncated protein that cannot bind to the leptin receptor anymore [1]. Therefore, although we cannot be sure that our mutant has a complete null phenotype, it is very likely that our truncation in the *lepb* gene leads to a leptin b protein which cannot bind to the leptin receptor in the zebrafish.

The $lepb^{+/+}$ and $lepb^{-/-}$ zebrafish are obtained from an incross of *lepb* heterozygous fish ($lep^{+/-}$); (Supplementary Fig. 1C). $Lepb^{+/+}$, $lepb^{+/-}$ and $lepb^{-/-}$ zebrafish were mixed and raised in the same tank before genotyping. After genotyping, $lepb^{+/+}$, $lepb^{+/-}$ and $lepb^{-/-}$ fish were separated

and raised in different sizes of tanks depending on the number of fish per volume of water. The ABTL (control) fish of 1.5 years old were kept in the big-sized-tanks. We raised all zebrafish in the same circulating water system and maintained the normal mixed-sex environment. Adult zebrafish were fed twice per day. One meal is a mixture of GEMMA Micro 300 and GEMMA Diamond (Skretting; Nutreco company) whose amount is based on 5% of zebrafish body weight; another is the life Artemia (ZebCare). Both amounts are positively proportional to the number of fish per tank and given by highly skilled caretakers.

We included both *lepb*$^{7-/7-}$ and *lepb*$^{8-/8-}$ mutants in the current study since two independent mutants have more certainty to rule out off-target effects of CRISPR-CAS9 approach. The age-matched ABTL adult zebrafish of the same lineage as used for the CRISPR-CAS9 procedure were used as the controls. In an independent study, a wild type (*lepb*$^{+/+}$) from an incross of heterozygotes *lepb*$^{7+/-}$ was compared with the ABTL control, showing no significant difference in blood glucose levels (Supplementary Fig. 2; female: $t_{(3)}$=-0.149, p=0.891; male: $t_{(3)}$=-2.820, p=0.067), further excluding off-target effects of the CRISPR-CAS9 procedure. For the current study, adult zebrafish (ABTL female fish, n=9; *lepb*$^{-/-}$ female fish, n=11; ABTL male fish, n=9; *lepb*$^{-/-}$ male fish, n=15) were sacrificed at the age of 1.5 years, since we observed that all *lepb*$^{-/-}$ mutants displayed an obese phenotype, compared to control zebrafish. Because there was no difference in body weight, body length, body mass index (BMI), and 2 hours postprandial blood glucose levels between *lepb*$^{7-/7-}$, *lepb*$^{8-/8-}$ and *lepb*$^{7-/8-}$ mutants (Supplementary Fig. 3), we pooled *lepb*$^{7-/7-}$, *lepb*$^{8-/8-}$ and *lepb*$^{7-/8-}$ mutants into one group which is named as *lepb*$^{-/-}$ for the subsequent analyses.

Body weight and body length measurement

Two hours after feeding, fish were sacrificed by putting them into ice-cold aquarium water which was filled with some ice chips to maintain the temperature near 0°C for 3-6 s. After there was no response of the fish to external stimuli, the euthanized fish was placed on a paper tissue, drying the body as much as possible. Then, the fish size (from the tip of the mouth to the caudal peduncle) was measured with a calliper, and the fish were weighed with a precision analytical scale.

Blood collection

A steel blade was used to cut the fish between anal fin and caudal fin just after euthanasia to collect zebrafish blood. The blood was collected into a 500µl Eppendorf tube with a 20 µl micro-pipet. Following the blood collection, the remaining body of the zebrafish was fixed in

4% paraformaldehyde (PFA). After 2 hours of coagulation at room temperature, the blood was spun down in a centrifuge at 13,000 g for 10 minutes. Subsequently, the blood serum and the blood cells were separated into different Eppendorf tubes and kept at -80°C for further analysis.

Blood glucose level measurement

A PicoProbe^{TM} Glucose Fluorometric Assay kit (Biovision, Milpitas, CA) was used to measure the glucose levels in the serum of zebrafish. The serum samples were diluted 50 times with milli-Q water. Nine µl of the diluted serum was added into a 96-well white plate, and then the total volume was adjusted to 50µl with 36µl glucose assay buffer and 5µl reaction mix which was composed of 0.5µl PicoProbe^{TM}, 1µl glucose substrate mix, 1µl glucose enzyme mix and 2.5µl glucose assay buffer. The 100mM glucose standard was diluted into a series of wells in 96 well plates to generate 0, 1.5, 3, 6, 9, 12, 15 micromolar per well for making the glucose standard curve. The volumes of different concentrations of glucose standards were also adjusted to 50µl with glucose assay buffer and reaction mix. The samples were incubated for 30 minutes at 37°C, protected from light. Fluorescence was measured at Excitation/Emission =535/587 nm in a microtiter plate reader. The concentrations of glucose in the serum of zebrafish were calculated according to the glucose standard curve.

MRI measurement

After one week fixation in 4% PFA at 4ºC, the whole adult fish were washed twice with PBS and then transferred to MR silent liquid (Fomblin, perfluoropolyether) for MRI measurement. All MR imaging scans were performed at 300 MHz Bruker vertical wide-bore system, using a birdcage radiofrequency coil with an inner diameter of 10 mm. Data acquisition and processing were performed with Para Vision 5.1 (Bruker Biospin, Germany). Before each measurement, the magnetic field homogeneity was optimized by shimming. Each session of measurements began with a multi-slice orthogonal gradient-echo sequence for position determination and selection of the desired region for subsequent experiments.

For anatomical images, a rapid acquisition with relaxation enhancement (RARE) sequences was used. Basic measurement parameters used for the RARE sequence were: Echo time (TE)=8.5 ms with an effective echo time of 18.1 ms; Repetition time (TR)=3000 ms; Number of scans (ns)=12; Total scan time= 17 min. RARE factor=4. The field of view (FOV) was 1.2 cm with a matrix size of 256 x 256, the slice thickness was 0.2 mm, and the interslice distance was also 0.2 mm.

For selective fat imaging, a Chemical Shift Selective (CHESS) sequence was used. The CHESS consists of a single frequency-selective excitation pulse with a flip angle of π/2 followed by a dephasing gradient (homogeneity spoiling gradient). The procedure leaves the spin system in a state where no net magnetization of the unwanted component is retained while the wanted component remains entirely unaffected in the form of z-magnetization. A narrow bandwidth of 90 degree Gaussian pulse was used for on resonance frequency selective excitation. Further basic parameters used are as follows: TE=13.3 ms; TR=800 ms; ns=16; Scan time 27 min.

For quantitative analysis of fat in CHESS images, the image slices were exported and analyzed in ImageJ software (https:// imagej.nih.gov/ij/). By using a plugin, the area of the fish was defined, and a certain threshold was adjusted to eliminate any contribution of noise. Subsequently, the hyperintense signal of fat was calculated. The data were exported to Origin Pro v. 8 software for further analysis.

Renal histopathology

After 1 week fixation in 4% PFA at 4°C, the whole adult zebrafish were washed twice with PBS and then transferred to EDTA (100mM, pH=8) for the decalcification at room temperature for another 1 week, followed by embedding in paraffin. The zebrafish tissue was cut (4-µm thickness) on a Leica microtome (Wetzlar) and then stained with HE or PAS using standard protocols.

Stained slides were digitalized using a Philips Ultra-Fast Scanner 1.6 RA (Philips Electronics, Amsterdam, the Netherlands). The surface areas (μm^2) of Bowman's capsule, Bowman's space, and glomerular tuft were measured in the digitalized PAS-stained slides using ImageJ software. All available glomeruli (5~11 glomeruli per slide) in each zebrafish were included in the measurements.

Transmission electron microscopy (TEM)

Zebrafish kidneys were harvested and fixed in EM fixation buffer (1.5% G.A/ 1% PF) for 24 hours. Subsequently, the renal tissue was fixed with 2.5% glutaraldehyde/1.2% acrolein in fixation buffer (0.1 mol/l cacodylate, 0.1 mol/l sucrose, pH 7.4) and 1% osmium tetroxide, and embedded in epon resin. Ultrathin sections were stained with uranyl acetate. The images were collected using a JEM-1200 EX transmission electron microscope (JEOL, Tokyo, Japan).

The thickness of the glomerular basement membrane (GBM) of zebrafish was analyzed with ImageJ software. One glomerulus per fish was analyzed. Photos of eight distinct areas (25.000X) of the glomerular capillaries from each glomerulus at randomly selected places were taken. The

mean thickness of the GBM in each photograph was determined by measuring the thickness of 15 nonoverlapping places of the GBM area. The mean of these 8 distinct areas was taken as the thickness for each glomerulus.

Statistical analyses

Statistical analysis was performed using SPSS Statistics 25 (IBM, Armonk, NY). Differences between groups were analyzed using Student's *t*-test. Data are presented as the mean ± SD. Differences with $p<0.05$ were considered as statistically significant.

Results

Deficiency of *lepb* has an effect on body weight, length and blood glucose levels in adult zebrafish

In this study, we first examined the basic parameters, including body weight, length and blood glucose levels, in control and *lepb*$^{-/-}$ adult zebrafish in both genders at the age of 1.5 years. The body weight of *lepb*$^{-/-}$ zebrafish in both genders was significantly increased compared to their respective controls (Fig. 1A; female: $t_{(8.191)}$=4.219, p=0.003; male: $t_{(16)}$=2.396, p=0.029). Accordingly, the body length of *lepb*$^{-/-}$ zebrafish was also significantly increased compared to the controls, in both genders (Fig. 1B; female: $t_{(12)}$= 2.680, p=0.020; male: $t_{(16)}$=3.266, p=0.005). Two hours postprandial blood glucose levels (Fig. 1C; female: $t_{(12)}$=0.357, p=0.727; male: $t_{(14)}$=2,230, p=0.043) and fasting blood glucose levels (Supplementary Fig. 4; female: $t_{(4)}$=0.999, p=0.374; male: $t_{(4)}$=3.289, p=0.030) in *lepb*$^{-/-}$ male zebrafish group were significantly higher compared to control male zebrafish group, but we did not find that in the female group.

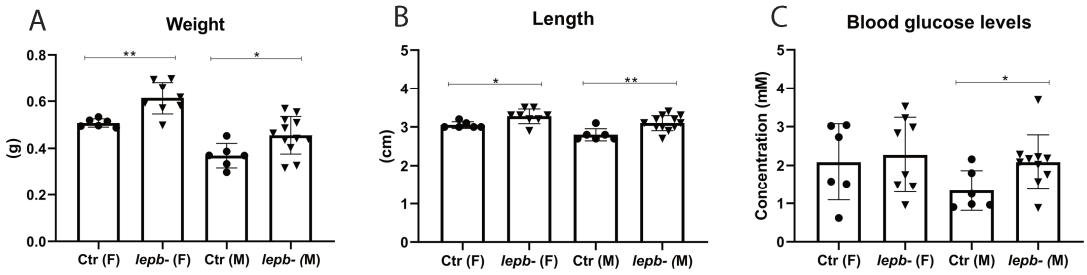


Figure 1. Body weight, length and blood glucose levels in control and *lepb*-deficient adult zebrafish
(A) The body weight of control and *lepb*$^{-/-}$ female (**p<0.01) and male (*p<0.05) adult zebrafish. (B) The body length of control and *lepb*$^{-/-}$ female (*p<0.05) and male (**p<0.01) adult zebrafish. (C) Two hours postprandial blood glucose levels in control and *lepb*$^{-/-}$ female and male (*p<0.05) adult zebrafish. Ctr: control zebrafish; *lepb*-: *lepb*$^{-/-}$ zebrafish; F: female; M: male.

Lepb-deficient adult zebrafish have more visceral fat accumulation

After observing the obese phenotype in *lepb*$^{-/-}$ zebrafish, we examined the body fat distribution in zebrafish with a non-invasive MRI approach. Successive slices were imaged from top to bottom in the coronal plane of control and *lepb*$^{-/-}$ zebrafish in both genders (Fig. 2). We observed a substantial increase in visceral fat accumulation in both *lepb*$^{-/-}$ female (Fig. 2B) and male (Fig. 2D) zebrafish compared to control female (Fig. 2A) and male (Fig. 2C) zebrafish. Furthermore, we performed the chemical shift selective (CHESS) imaging to acquire clear fat distribution images (Fig. 2A'-D'). A quantitative analysis of body fat from CHESS images clearly showed

a significant increase in fat accumulation in *lepb*$^{-/-}$ zebrafish in both genders compared to their respective controls (Fig. 2E; female: $t_{(10)}$=7.057, p<0.001; male: $t_{(10)}$=5.231, p<0.001).

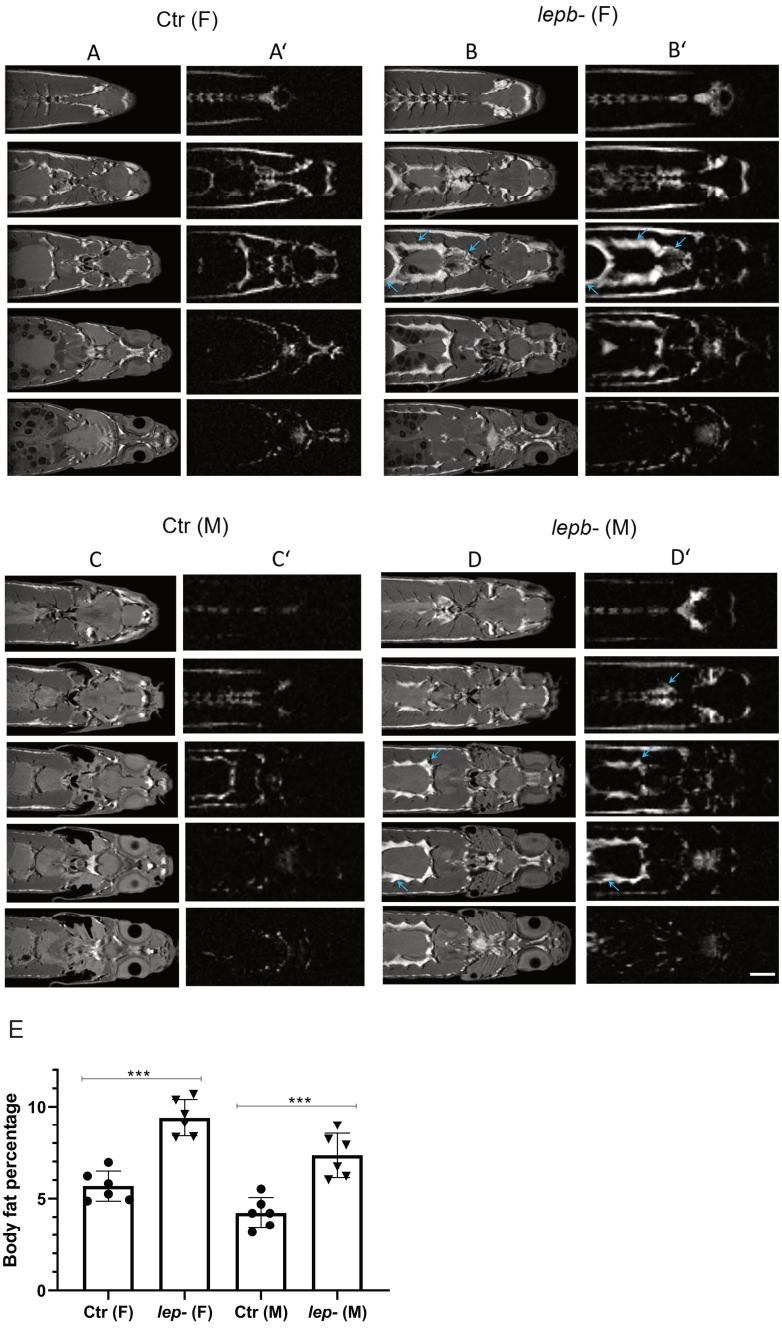


Figure 2. Magnetic resonance anatomical imaging and selective fat imaging in control and *lepb*-deficient female and male adult zebrafish

(A-D) Successive slices (top to bottom) in the coronal plane obtained using T_2 weighted RARE pulse sequence. (A'-D') Successive images (top to bottom) of fat distribution in the coronal plane, acquired with Chemical Shift Selective (CHESS) pulse sequence. (A, A') Control female; (B, B') *lepb*$^{-/-}$ female;

(C, C') Control male; (D, D') *lepb*$^{-/-}$ male adult zebrafish. A substantial visceral fat accumulation was seen in *lepb*$^{-/-}$ adult zebrafish (arrow) as compared to control adult zebrafish (female and male). Scale bar: 2.5 mm. (E) Quantification of body fat in control and *lepb*$^{-/-}$ female (***p<0.001) and male (***p<0.001) adult zebrafish was measured from CHESS MR images. Ctr: control zebrafish; *lepb*-: *lepb*$^{-/-}$ zebrafish; F: female; M: male.

Lepb-deficient male adult zebrafish develop glomerular hypertrophy

Subsequently, we investigated the histopathology of the zebrafish kidney, an organ with a high vulnerability under the diabetic condition. We found a substantial increase in the surface area of the glomeruli of *lepb*$^{-/-}$ male zebrafish (Fig. 3B), compared to control male zebrafish (Fig. 3A), on PAS-stained slides. A quantitative analysis of the surface area of the glomeruli showed significant enlargement of Bowman's capsule (Fig. 3C; $t_{(13)}$=3.725, p=0.003) and glomerular tuft (Fig. 3D; $t_{(13)}$=3.176, p=0.007) in *lepb*$^{-/-}$ male zebrafish compared to control male zebrafish, indicating that *lepb*$^{-/-}$ male zebrafish develop glomerular hypertrophy. The surface area of Bowman's space was also larger in *lepb*$^{-/-}$ male zebrafish compared to controls. However, this difference did not reach statistical significance (Fig. 3E; $t_{(13)}$=2.108, p=0.055).

Besides, we did not observe severe mesangial matrix expansion in the glomeruli of *lepb*$^{-/-}$ male zebrafish. Tubular injury and interstitial fibrosis, the final events of chronic tubular injury, contribute to the loss of kidney function. The tubular histology of *lepb*$^{-/-}$ male zebrafish was as normal as control male zebrafish on both PAS- (Fig. 3A and 3B) and HE- stained slides (Fig. 3F and 3G), and no signs of the tubular atrophy and interstitial fibrosis were observed.

Lepb-deficient male adult zebrafish show a thickening of the GBM

Thickening of the GBM is an early sign of diabetic nephropathy (DN). We found a significant increase (2.6 times) in the thickness of GBM in *lepb*$^{-/-}$ male zebrafish (Fig. 4A-4D, and 4H; $t_{(4)}$=10.281, p=0.001) compared to controls via TEM approach.

Furthermore, we observed some fibers surrounding the GBM in the glomeruli of *lepb*$^{-/-}$ male zebrafish (Fig. 4G), suggesting there might have the extracellular matrix accumulation. However, we did not observe obvious podocyte foot process effacement and endothelial cell damage in the glomeruli of *lepb*$^{-/-}$ male zebrafish. Besides, the ultrastructure of the renal proximal tubules of *lepb*$^{-/-}$ male zebrafish was normal and indistinguishable when comparing to control male zebrafish (Fig. 4E and 4F), which is consistent with the findings from HE and PAS staining.

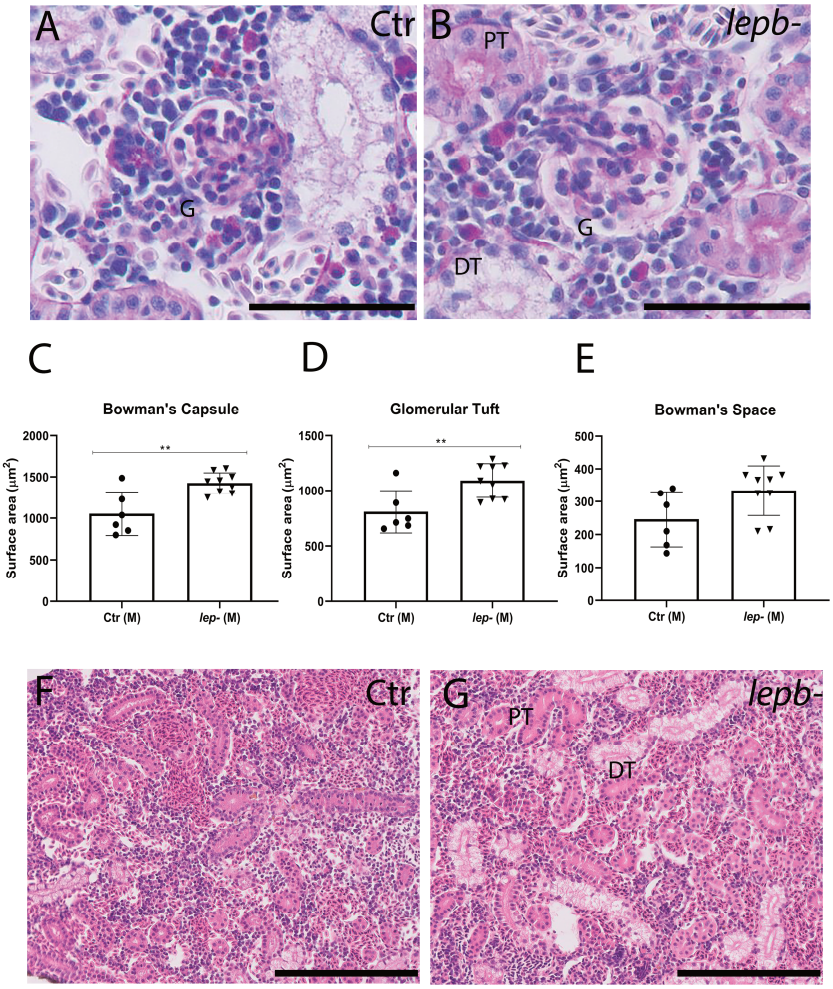


Figure 3. *Lepb*-deficient male adult zebrafish develop glomerular hypertrophy

(A-B) Representative images of the glomeruli of control (A) and *lepb*$^{-/-}$ (B) male adult zebrafish; the scale bars represent 50µm; PAS staining. (C) Summary of the surface areas of Bowman's capsule of control and *lepb*$^{-/-}$ male adult zebrafish (**p<0.01). (D) Summary of the surface areas of Glomerular tuft of control and *lepb*$^{-/-}$ male adult zebrafish (**p<0.01). (E) Summary of the surface areas of Bowman's space of control and *lepb*$^{-/-}$ male adult zebrafish. (F-G) Representative images of the tubules of control (F) and *lepb*$^{-/-}$ (G) male adult zebrafish; the scale bars represent 50µm; HE staining. Ctr: control zebrafish; *lepb*-: *lepb*$^{-/-}$ zebrafish; M: male; G: glomeruli; PT: proximal tubule; DT: distal tubule.

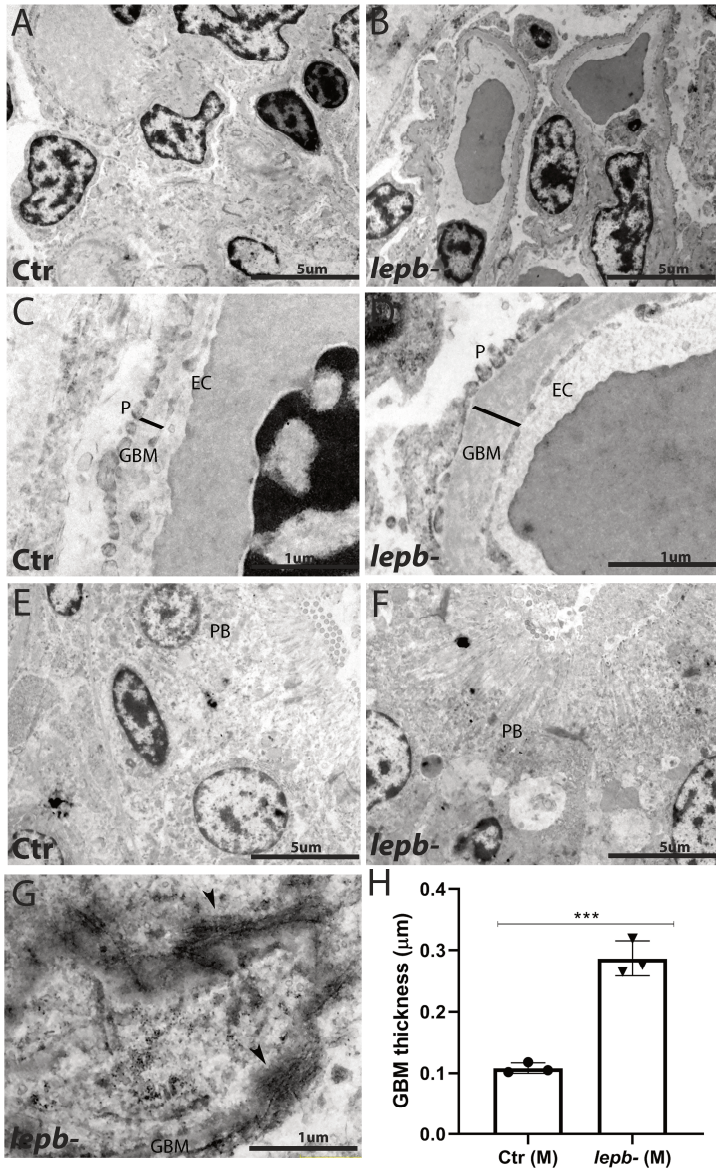


Figure 4. Transmission electron microscopy pictures of glomeruli and tubules from control and *lepb*-deficient male adult zebrafish

(A-B) Representative images of glomeruli from control (A) and *lepb*$^{-/-}$ (B) male adult zebrafish; magnification 5000X. (C-D) High magnification view of one segment of a glomerular capillary from control (C) and *lepb*$^{-/-}$ (D) male adult zebrafish (the thickness of GBM was marked by black lines); magnification 25.000X. (E-F) Representative images of the tubular brash border of the proximal tubule of control (E) and *lepb*$^{-/-}$ (F) male adult zebrafish; magnification 5000X. (G) High magnification of the fibrillar mesangial matrix in *lepb*$^{-/-}$ male adult zebrafish (black arrowheads); magnification 50.000X. (H) Summary of the thickness of GBM in the control and *lepb*$^{-/-}$ male adult zebrafish. The thickness of GBM in *lepb*$^{-/-}$ male zebrafish is 2.6 times thicker than that in control male zebrafish (**p<0.01). Ctr: control zebrafish; *lepb*-: *lepb*$^{-/-}$ zebrafish; M: male; GBM: glomerular basement membrane; P: podocytes; EC: endothelial cells; PB: proximal tubular brush border.

Discussion

In the current study, we generated *lepb*-deficient zebrafish by using the CRISPR/CAS9 gene editing approach. We demonstrated that 1.5 years old *lepb*$^{-/-}$ adult zebrafish in both genders had an increase in body weight, length and visceral fat accumulation compared to their respective controls. Furthermore, we found that the blood glucose levels in *lepb*$^{-/-}$ male adult zebrafish were significantly higher than control male adult zebrafish. Lastly, we showed that *lepb*$^{-/-}$ male adult zebrafish developed early signs of DN.

There are conflicting reports whether the disruption of leptin signaling induces adiposity in zebrafish. Audira et al. reported that *lepa*-deficient adult zebrafish display an obese phenotype [26]. On the other hand, Michel et al. [24] did not detect an increased fat mass or higher body weight in *lepr*-deficient adult zebrafish. In the current study, we observed that all *lepb* mutants had an increased body weight and body length compared to controls at the adult stage. However, no difference in BMI between control and *lepb*$^{-/-}$ zebrafish, in both genders, was found (Supplementary Fig. 3C; female: $t_{(12)}$=1.120, p=0.285; male: $t_{(16)}$=0.070, p=0.945). It is well known that increased visceral fat accumulation is a typical feature of obesity. In addition, it has been suggested in the literature that body fat percentage and visceral fat level can predict type II diabetes [28] or insulin resistance [29] better than BMI. To more precisely compare the body fat distribution between control and *lepb*$^{-/-}$ zebrafish, the successive slices from top to bottom in the coronal plane were imaged via an MRI approach. We found a significantly increased visceral fat accumulation in the *lepb*$^{-/-}$ zebrafish compared to control zebrafish in both genders. The increase of body weight and visceral fat accumulation in *lepb*$^{-/-}$ zebrafish in both genders jointly suggested that *lepb* deficiency results in adiposity in zebrafish. How can we reconcile our findings with the study of Michel et al. [24] showing that *lepr*-deficient zebrafish did not develop obesity? The different findings between these two studies might be due to the different age of zebrafish investigated, or different feeding protocols. Alternatively, leptin signaling in zebrafish might also have functions that are independent of the leptin receptor. Besides, to exclude off-target effects in our study, we investigated three different mutants, including *lepb*$^{7-/7-}$, *lep*$^{8-/8-}$ and *lepb*$^{7-/8-}$ mutants, in the *lepb*-deficient (*lepb*$^{-/-}$) group. We found that all these three mutants of *lepb*$^{-/-}$ adult zebrafish had an increased body weight and body length, compared to the controls, which makes it unlikely that our results are caused by the off-target effects of the CRISPR-CAS9 procedure.

Recently, researchers have generated different diabetic models in zebrafish. For instance, Zhang et al. developed a zebrafish model for T2DM by overfeeding 4~6 months old fish with diet-induced obesity (DIO) food over 8 weeks, and they showed that these obese fish have

increased fasting blood glucose levels [30]. Olsen et al. induced a type 1 diabetes mellitus (T1DM) in 4~6 months old zebrafish by injecting streptozotocin (STZ) to ablate beta cells from the pancreas [31]. This STZ-induced T1DM zebrafish model represents several diabetic complications, such as retinal thinning (an early sign of retinopathy) and GBM thickening (an early sign of nephropathy). However, to further investigate diabetes in zebrafish, there is still a lack of a congenital diabetic zebrafish line which does not require time-consuming feeding schemes or invasive procedures which might cause side effects when induces the diabetic symptoms.

Diabetes is characterised by hyperglycemia which plays a crucial role in the development of diabetes complications. In the current study, we found that 2 hours postprandial blood glucose levels and fasting blood glucose levels of *lepb*$^{-/-}$ male zebrafish were significantly higher than the levels of control male zebrafish. However, we did not detect this difference in female zebrafish. A review from Wang et al. illustrated that diabetic manifestations in some of the rodent models do not develop in females or are not as apparent as in males [32]. Therefore, it is very interesting that we got similar results in the current study in a fish model. The increased body weight, length and visceral fat accumulation and higher blood glucose levels in *lepb*$^{-/-}$ male zebrafish collectively indicate that *lepb*-deficient male adult zebrafish display the features of T2DM. To further explore the glucose homeostasis in the *lepb*-deficient zebrafish model, it would be very interesting to investigate whether the whole-body glucose level has already increased in the *lepb*-deficient zebrafish at the larvae stage.

Growing literature provides evidence that leptin has a glucose-lowering effect. A previous study reported that the infusion of leptin into the brain could normalize the hyperglycemia in *ob/ob* mice [33]. Insulin has a robust role in the regulation of glucose homeostasis, and insulin resistance is a fundamental aspect of the etiology of T2DM. Several studies have demonstrated that leptin can improve insulin sensitivity [18,34]. An experimental study from Morton et al. suggested that reduced leptin in the mediobasal hypothalamus leads to severe insulin resistance and glucose intolerance in Koletsky rats, and phosphatidylinositol-3-OH kinase signaling is a vital mediator of this effect [35]. In addition, Yu et al. reported that leptin could reverse the hyperglycemia and ketosis by suppressing the action of glucagon on the liver and improving the utilization of glucose in the skeletal muscle in insulin-deficient diabetic rodents [11]. These studies indicated that leptin acts on glucose metabolism in both insulin-dependent and insulin-independent ways. Earlier work from our laboratory had demonstrated that *lepb* was significantly downregulated in zebrafish larvae under an insulin-resistance state [27]. Future studies should investigate whether the diabetic phenotype of *lepb* mutants is caused by disruption of the insulin signaling pathway.

The segmental anatomy of the nephron is conserved among the vertebrates [36]. Olsen et al. found that STZ-induced T1DM zebrafish have a thickening of the GBM (an early sign of DN) [31]. In the current study, we want to address whether *lepb*$^{-/-}$ adult zebrafish develop DN or not. We found the *lepb*$^{-/-}$ male group had higher blood glucose levels compared to the control male group, but not in the female group. Therefore, the kidney in male zebrafish was further investigated by performing histopathological examination. Glomerular hypertrophy, mesangial expansion, and thickening of the GBM are the particular characteristics of the histopathology of DN [37]. We found that *lepb*$^{-/-}$ male zebrafish develop glomerular hypertrophy and thickening of the GBM, compared to control male zebrafish. However, we did not observe severe mesangial expansion, podocyte damage, or tubular cell damage in the kidney tissue of *lepb*$^{-/-}$ male zebrafish. These findings collectively indicate that the renal injury in *lepb*$^{-/-}$ male zebrafish is relatively mild.

In summary, we demonstrated that *lepb* regulates glucose homeostasis and adiposity in zebrafish, and deletion of the *lepb* gene results in the development of T2DM and the early stage of DN. These results suggest that *lepb*-deficient zebrafish can be used as a T2DM model, and further investigation would give us new insights into the mechanistic function of leptin in T2DM.

Declaration of interest

All authors declare no competing interests.

Funding

The work was supported by the Polish National Science Center (grant number 2016/21/N/NZ6/01162).

Acknowledgements

The first authors (J. He and Y. Ding) were supported by the China Scholarship Council (CSC). We would like to thank Peter Neeskens for the technical support of the transmission electron microscopy (TEM).

References

1 Zhang, Y. *et al.* Positional cloning of the mouse obese gene and its human homologue. *Nature* **372**, 425-432, doi:10.1038/372425a0 (1994).

2 Ahima, R. S., Prabakaran, D. & Flier, J. S. Postnatal leptin surge and regulation of circadian rhythm of leptin by feeding. Implications for energy homeostasis and neuroendocrine function. *The Journal of clinical investigation* **101**, 1020-1027, doi:10.1172/JCI1176 (1998).

3 Lord, G. M. *et al.* Leptin modulates the T-cell immune response and reverses starvation-induced immunosuppression. *Nature* **394**, 897-901, doi:10.1038/29795 (1998).

4 Matarese, G., Moschos, S. & Mantzoros, C. S. Leptin in immunology. *J Immunol* **174**, 3137-3142, doi:10.4049/jimmunol.174.6.3137 (2005).

5 Meier, U. & Gressner, A. M. Endocrine regulation of energy metabolism: review of pathobiochemical and clinical chemical aspects of leptin, ghrelin, adiponectin, and resistin. *Clin Chem* **50**, 1511-1525, doi:10.1373/clinchem.2004.032482 (2004).

6 Caprio, M., Fabbrini, E., Isidori, A. M., Aversa, A. & Fabbri, A. Leptin in reproduction. *Trends Endocrinol Metab* **12**, 65-72, doi:10.1016/s1043-2760(00)00352-0 (2001).

7 Licinio, J. *et al.* Phenotypic effects of leptin replacement on morbid obesity, diabetes mellitus, hypogonadism, and behavior in leptin-deficient adults. *Proc Natl Acad Sci U S A* **101**, 4531-4536, doi:10.1073/pnas.0308767101 (2004).

8 Farooqi, I. S. *et al.* Effects of recombinant leptin therapy in a child with congenital leptin deficiency. *N Engl J Med* **341**, 879-884, doi:10.1056/NEJM199909163411204 (1999).

9 Funcke, J. B. *et al.* Monogenic forms of childhood obesity due to mutations in the leptin gene. *Mol Cell Pediatr* **1**, 3, doi:10.1186/s40348-014-0003-1 (2014).

10 Drel, V. R. *et al.* The leptin-deficient (ob/ob) mouse: a new animal model of peripheral neuropathy of type 2 diabetes and obesity. *Diabetes* **55**, 3335-3343, doi:10.2337/db06-0885 (2006).

11 Yu, X., Park, B. H., Wang, M. Y., Wang, Z. V. & Unger, R. H. Making insulin-deficient type 1 diabetic rodents thrive without insulin. *Proc Natl Acad Sci U S A* **105**, 14070-14075, doi:10.1073/pnas.0806993105 (2008).

12 Fujikawa, T., Chuang, J. C., Sakata, I., Ramadori, G. & Coppari, R. Leptin therapy improves insulin-deficient type 1 diabetes by CNS-dependent mechanisms in mice. *Proc Natl Acad Sci U S A* **107**, 17391-17396, doi:10.1073/pnas.1008025107 (2010).

13 Hedbacker, K. *et al.* Antidiabetic effects of IGFBP2, a leptin-regulated gene. *Cell Metab* **11**, 11-22, doi:10.1016/j.cmet.2009.11.007 (2010).

14 German, J. P. *et al.* Leptin activates a novel CNS mechanism for insulin-independent normalization of severe diabetic hyperglycemia. *Endocrinology* **152**, 394-404, doi:10.1210/en.2010-0890 (2011).

15 Muzzin, P., Eisensmith, R. C., Copeland, K. C. & Woo, S. L. Correction of obesity and diabetes in genetically obese mice by leptin gene therapy. *Proc Natl Acad Sci U S A* **93**, 14804-14808, doi:10.1073/pnas.93.25.14804 (1996).

16 Pocai, A. *et al.* Central leptin acutely reverses diet-induced hepatic insulin resistance. *Diabetes* **54**, 3182-3189, doi:10.2337/diabetes.54.11.3182 (2005).

17 Park, S., Hong, S. M., Sung, S. R. & Jung, H. K. Long-term effects of central leptin and resistin on body weight, insulin resistance, and beta-cell function and mass by the modulation of hypothalamic leptin and insulin signaling. *Endocrinology* **149**, 445-454, doi:10.1210/en.2007-0754 (2008).

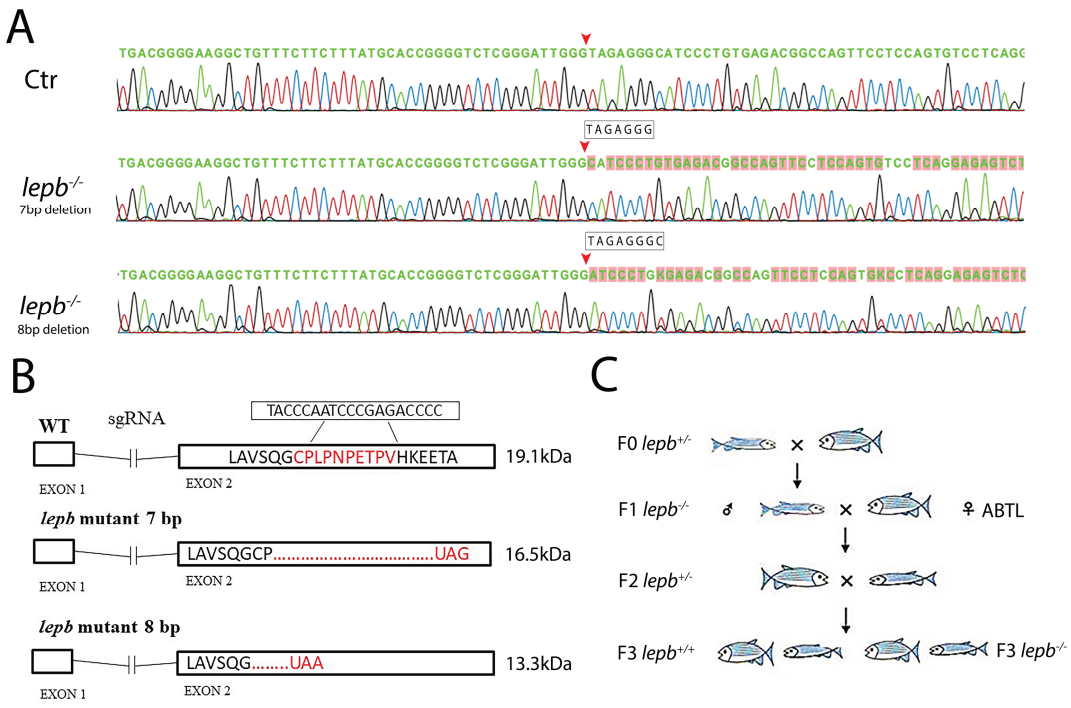
18 German, J. *et al.* Hypothalamic leptin signaling regulates hepatic insulin sensitivity via a neurocircuit involving the vagus nerve. *Endocrinology* **150**, 4502-4511, doi:10.1210/en.2009-0445 (2009).

19 Denver, R. J., Bonett, R. M. & Boorse, G. C. Evolution of leptin structure and function. *Neuroendocrinology* **94**, 21-38, doi:10.1159/000328435 (2011).

20 Volkoff, H., Eykelbosh, A. J. & Peter, R. E. Role of leptin in the control of feeding of goldfish Carassius auratus: interactions with cholecystokinin, neuropeptide Y and orexin A, and modulation by fasting. *Brain Res* **972**, 90-109, doi:10.1016/s0006-8993(03)02507-1 (2003).

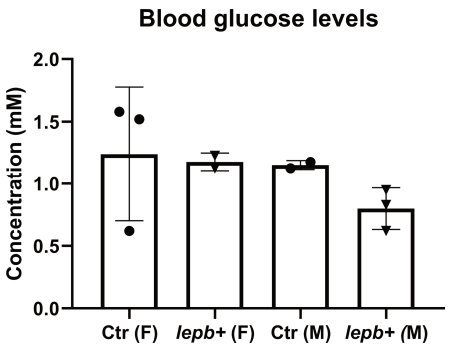
21 Murashita, K., Uji, S., Yamamoto, T., Ronnestad, I. & Kurokawa, T. Production of recombinant leptin and its effects on food intake in rainbow trout (Oncorhynchus mykiss). *Comp Biochem Physiol B Biochem Mol Biol* **150**, 377-384, doi:10.1016/j.cbpb.2008.04.007 (2008).
22 Aguilar, A. J., Conde-Sieira, M., Lopez-Patino, M. A., Miguez, J. M. & Soengas, J. L. In vitro leptin treatment of rainbow trout hypothalamus and hindbrain affects glucosensing and gene expression of neuropeptides involved in food intake regulation. *Peptides* **32**, 232-240, doi:10.1016/j.peptides.2010.11.007 (2011).
23 Gorissen, M., Bernier, N. J., Nabuurs, S. B., Flik, G. & Huising, M. O. Two divergent leptin paralogues in zebrafish (Danio rerio) that originate early in teleostean evolution. *The Journal of endocrinology* **201**, 329-339, doi:10.1677/JOE-09-0034 (2009).
24 Michel, M., Page-McCaw, P. S., Chen, W. & Cone, R. D. Leptin signaling regulates glucose homeostasis, but not adipostasis, in the zebrafish. *Proc Natl Acad Sci U S A* **113**, 3084-3089, doi:10.1073/pnas.1513212113 (2016).
25 Chisada, S. *et al.* Leptin receptor-deficient (knockout) medaka, Oryzias latipes, show chronical up-regulated levels of orexigenic neuropeptides, elevated food intake and stage specific effects on growth and fat allocation. *Gen Comp Endocrinol* **195**, 9-20 (2014).
26 Audira, G. *et al.* Zebrafish Mutants Carrying Leptin a (lepa) Gene Deficiency Display Obesity, Anxiety, Less Aggression and Fear, and Circadian Rhythm and Color Preference Dysregulation. *Int J Mol Sci* **19**, doi:10.3390/ijms19124038 (2018).
27 Marin-Juez, R., Jong-Raadsen, S., Yang, S. & Spaink, H. P. Hyperinsulinemia induces insulin resistance and immune suppression via Ptpn6/Shp1 in zebrafish. *The Journal of endocrinology* **222**, 229-241, doi:10.1530/JOE-14-0178 (2014).
28 Lebovitz, H. E. & Banerji, M. A. Point: visceral adiposity is causally related to insulin resistance. *Diabetes Care* **28**, 2322-2325, doi:10.2337/diacare.28.9.2322 (2005).
29 Kurniawan, L. B., Bahrun, U., Hatta, M. & Arif, M. Body Mass, Total Body Fat Percentage, and Visceral Fat Level Predict Insulin Resistance Better Than Waist Circumference and Body Mass Index in Healthy Young Male Adults in Indonesia. *J Clin Med* **7**, doi:10.3390/jcm7050096 (2018).
30 Zang, L., Shimada, Y. & Nishimura, N. Development of a Novel Zebrafish Model for Type 2 Diabetes Mellitus. *Sci Rep* **7**, 1461, doi:10.1038/s41598-017-01432-w (2017).
31 Olsen, A. S., Sarras, M. P., Jr. & Intine, R. V. Limb regeneration is impaired in an adult zebrafish model of diabetes mellitus. *Wound Repair Regen* **18**, 532-542, doi:10.1111/j.1524-475X.2010.00613.x (2010).
32 Wang, B., Chandrasekera, P. C. & Pippin, J. J. Leptin- and leptin receptor-deficient rodent models: relevance for human type 2 diabetes. *Curr Diabetes Rev* **10**, 131-145, doi:10.2174/15733998106661405081210 12 (2014).
33 Kamohara, S., Burcelin, R., Halaas, J. L., Friedman, J. M. & Charron, M. J. Acute stimulation of glucose metabolism in mice by leptin treatment. *Nature* **389**, 374-377, doi:10.1038/38717 (1997).
34 Shimomura, I., Hammer, R. E., Ikemoto, S., Brown, M. S. & Goldstein, J. L. Leptin reverses insulin resistance and diabetes mellitus in mice with congenital lipodystrophy. *Nature* **401**, 73-76, doi:10.1038/43448 (1999).
35 Morton, G. J. *et al.* Leptin regulates insulin sensitivity via phosphatidylinositol-3-OH kinase signaling in mediobasal hypothalamic neurons. *Cell Metab* **2**, 411-420, doi:10.1016/j.cmet.2005.10.009 (2005).
36 McCampbell, K. K. & Wingert, R. A. New tides: using zebrafish to study renal regeneration. *Transl Res* **163**, 109-122, doi:10.1016/j.trsl.2013.10.003 (2014).
37 Tervaert, T. W. *et al.* Pathologic classification of diabetic nephropathy. *J Am Soc Nephrol* **21**, 556-563, doi:10.1681/ASN.2010010010 (2010).

Supplementary data



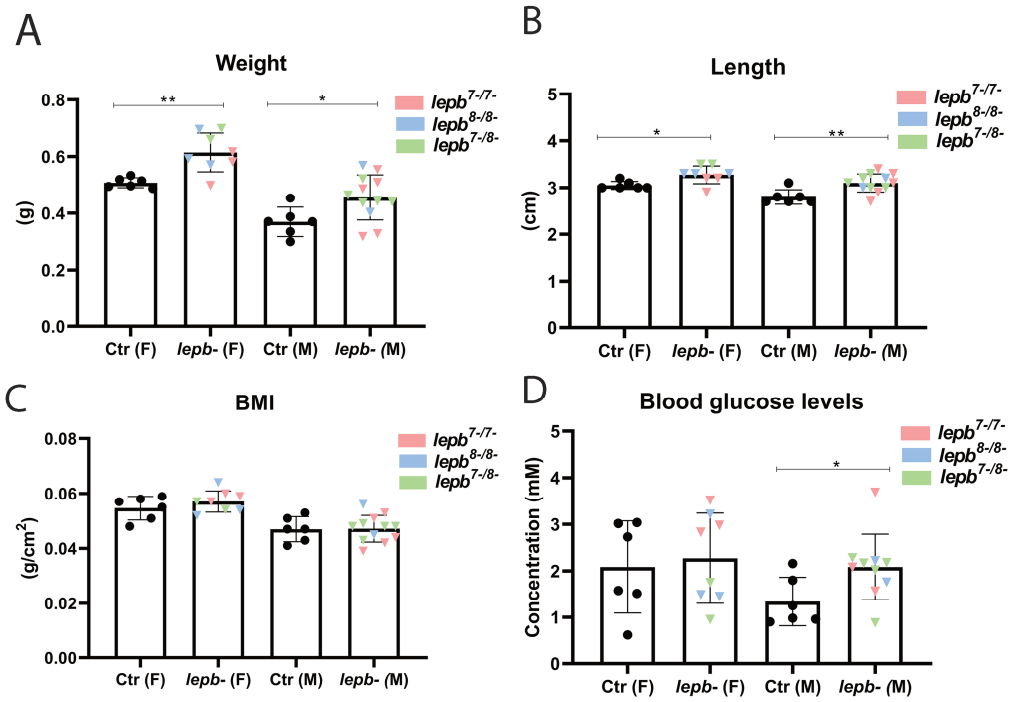
Supplementary Figure 1. Lepb-deficient zebrafish line

(A) The wild type zebrafish (Ctr) is showing a partial sequence of the *lepb* gene. Seven base pairs (TAGAGGG) were deleted in $lepb^{7-/7-}$ zebrafish and eight base pairs (TAGAGGGC) were deleted in $lepb^{8-/8-}$ zebrafish. The arrowheads show the start point of the deletion. (B) The wild type *lepb* gene translates into the predicted 19.1 kDa lepb protein in zebrafish. The seven base pairs deletion creates a premature stop codon UAG in exon 2, which results in a truncated 16.5 kDa protein. And the eight base pairs deletion causes a premature stop codon UAA in exon 2, which results in a truncated 13.3 kDa protein. (C) Homozygous F1 carriers were outcrossed once against the wild type zebrafish (ABTL) and the offspring (heterozygote $lepb^{+/-}$) were subsequently incrossed, resulting in the used $lepb^{+/+}$ and $lepb^{-/-}$ siblings. Because of the limitations of the number of adult zebrafish during this study, we used adult WT-ABTL (Ctr) and all $lepb^{-/-}$ ($lepb^{7-/7-}$, $lepb^{8-/8-}$ and $lepb^{7-/8-}$) for the experiments.



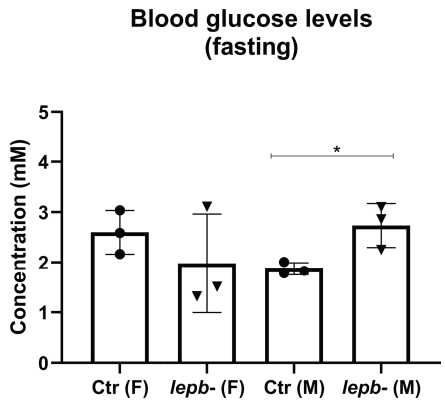
Supplementary Figure 2. Blood glucose levels in *lepb*$^{+/+}$ adult zebrafish and age-matched ABTL control zebrafish

Two hours postprandial blood glucose levels in ABTL control and *lepb*$^{+/+}$ zebrafish (female and male). Ctr: ABTL control zebrafish; *lepb*+: *lepb*$^{+/+}$ zebrafish; F: female; M: male.



Supplementary Figure 3. Body weight, length, BMI and blood glucose levels in different *lepb*$^{-/-}$ mutants

(A) The body weight of control and *lepb*$^{-/-}$ female (**p<0.01) and male (*p<0.05) adult zebrafish. (B) The body length of control and *lepb*$^{-/-}$ female (*p<0.05) and male (**p<0.01) adult zebrafish. (C) The BMI of control and *lepb*$^{-/-}$ female and male adult zebrafish. (D) Two hours postprandial blood glucose levels in control and *lepb*$^{-/-}$ female and male (*p<0.05) adult zebrafish. Different *lepb*$^{-/-}$ mutants were marked in different colors. *lepb*$^{7-/7-}$ in red, *lepb*$^{8-/8-}$ in blue and *lepb*$^{7-/8-}$ in green. Ctr: control zebrafish; *lepb*-: *lepb*$^{-/-}$ zebrafish; F: female; M: male.



Supplementary Figure 4. Fasting blood glucose levels in control and lepb-deficient adult zebrafish

Fasting blood glucose levels in control and *lepb*$^{-/-}$ female and male (*p<0.05) adult zebrafish. Ctr: control zebrafish; *lepb*-: *lepb*$^{-/-}$ zebrafish; F: female; M: male.